



Study of the reversible water vapour sorption process of $\text{MgSO}_4 \cdot 7\text{H}_2\text{O}$ and $\text{MgCl}_2 \cdot 6\text{H}_2\text{O}$ under the conditions of seasonal solar heat storage

C.J. Ferchaud

H.A. Zondag

J.B.J. Veldhuis

R. de Boer

*Presented at the 6th European Thermal Sciences Conference, Eurotherm 2012,
September 04 - 07, 2012, Poitiers - Futuroscope France*

Study of the reversible water vapour sorption process of $\text{MgSO}_4 \cdot 7\text{H}_2\text{O}$ and $\text{MgCl}_2 \cdot 6\text{H}_2\text{O}$ under the conditions of seasonal solar heat storage

CJ Ferchaud¹, HA Zondag^{1,2}, JBJ Veldhuis¹ and R de Boer¹

¹ ECN, Energy Research Centre of the Netherlands, P.O. Box 1, 1755 ZG Petten, NL

² Eindhoven University of Technology, Department of Mechanical Engineering, P.O. Box 513, 5600 MB Eindhoven, NL

E-mail: ferchaud@ecn.nl

Abstract. The characterization of the structural, compositional and thermodynamic properties of $\text{MgSO}_4 \cdot 7\text{H}_2\text{O}$ and $\text{MgCl}_2 \cdot 6\text{H}_2\text{O}$ has been done using *in-situ* X-ray Diffraction and thermal analyses (TG/DSC) under practical conditions for seasonal heat storage ($T_{\text{max}}=150^\circ\text{C}$, $p(\text{H}_2\text{O})=13$ mbar). This study showed that these two materials release heat after a dehydration/hydration cycle with energy densities of 0.38 GJ/m^3 for $\text{MgSO}_4 \cdot 7\text{H}_2\text{O}$ and 0.71 GJ/m^3 $\text{MgCl}_2 \cdot 6\text{H}_2\text{O}$. The low heat release found for $\text{MgSO}_4 \cdot 7\text{H}_2\text{O}$ is mainly attributed to the amorphization of the material during the dehydration performed at 13 mbar which reduces its sorption capacity during the rehydration. $\text{MgCl}_2 \cdot 6\text{H}_2\text{O}$ presents a high energy density which makes this material interesting for seasonal heat storage in domestic applications. This material would be able to fulfil the winter heat demand of a passive house estimated at 6 GJ with a packed bed reactor of 8.5 m^3 . However, a seasonal heat storage system built with this material should be carefully set with a restricted temperature at 40°C for the hydration reaction to avoid the liquefaction of the material at lower temperature which limits its performances for long term storage.

1. Introduction

The main part of the residential energy demand in Europe consists of space heating and domestic water heating. During summer, the available solar energy exceeds the domestic water heating demand for houses that are equipped with solar thermal collectors. However, during winter the total heating demand exceeds the solar supply. This mismatch can be solved by harvesting solar energy in summer to fulfil the heat demand in winter by means of a seasonal heat storage system. A passive house of 110 m^2 with a winter heat demand estimated at 6 GJ, seasonal heat storage in a traditional water tank would require a tank volume above 40 m^3 which is much too large to be integrated in individual houses. Therefore, more compact heat storage technologies have to be found. ECN develops a compact heat storage system based on the reversible reaction of water vapour in salt hydrates. These thermochemical (TCM) materials present a high energy density in packed bed ($\sim 1 \text{ GJ/m}^3$) resulting in a relatively small storage volume (around 6 m^3), that can easily be integrated in a house. Additionally, many salt hydrates are available in large quantity at low cost, are environmentally friendly and can take up and release heat under the conditions of seasonal heat storage. During summer, the salt hydrate materials can be dehydrated by means of solar heat provided by solar thermal collectors with a temperature below 150°C . During winter, the packed bed is rehydrated with moist air, e.g. by means

of the evaporation of water with low temperature heat from a borehole at 10°C, which defines the practical conditions for hydration in a TC seasonal storage system.

A screening of suitable materials has been performed in the last decade and several materials such as magnesium sulphate heptahydrate ($\text{MgSO}_4 \cdot 7\text{H}_2\text{O}$) and magnesium chloride hexahydrate ($\text{MgCl}_2 \cdot 6\text{H}_2\text{O}$) showed promising performances during tests in lab scale reactors under practical conditions of seasonal heat storage. However, their efficiency for long term storage can still be improved [1]. In order to develop an optimal sorption material for seasonal heat storage, ECN carried out a research project which aims at improving the heat storage system by designing a new optimized material with a high storage capacity, that remains stable over a lifetime of 30 years for the heat storage system. The first phase of the project is to identify the influence of the structural properties of these materials on the water vapour sorption process taking place during the dehydration and hydration reactions. To this end, powder samples of $\text{MgSO}_4 \cdot 7\text{H}_2\text{O}$ and $\text{MgCl}_2 \cdot 6\text{H}_2\text{O}$ have been studied under practical conditions by *in-situ* X-ray diffraction. In parallel, thermal analysis studies were performed on these two materials to identify the kinetics of reactions occurring during the water vapour sorption process. The present work reports the results obtained from these experiments.

2. Materials and methods

2.1. Materials

Pro Analyse reagent powders of magnesium sulphate heptahydrate (VWR BDH Prolabo, CAS 10034-99-8, NORMAPUR, 99.5% pure) and magnesium chloride hexahydrate (Merck, CAS 7791-48-6, $\geq 99\%$ pure) were used in this study. The powders were sieved prior to the experiments to obtain powders with different particle size ranges. Unless stated otherwise, particles with a particle size distribution ranging from 100 μm to 200 μm were used during the experiments. Powder samples of 10 mg were used in the different measurements performed in this study in order to avoid effects of layer thickness on vapour transport as shown in previous studies [2].

2.2. Settings of the practical conditions.

Each measurement in this study was carried out under well-controlled conditions for temperature and water vapour pressure, corresponding to practical conditions in the seasonal heat storage system. Depending on the type of characterization technique, the temperature was controlled either by local heating with hot-stage systems or trace heating with a furnace. Slow heating and cooling rates (0.2 - 1°C/min) were used during the different measurements in order to obtain experimental conditions as close as possible to the equilibrium conditions in the water vapour sorption process. Additionally, the vapour pressure was controlled by means of a well-controlled humidification system, shown in figure 1. This system was designed in order to perform a parallel control of the water vapour pressure and of the flow velocity in the system. These parameters were settled at 13 mbar (± 0.2 mbar) and at 100 ml/min (± 2 ml/min).

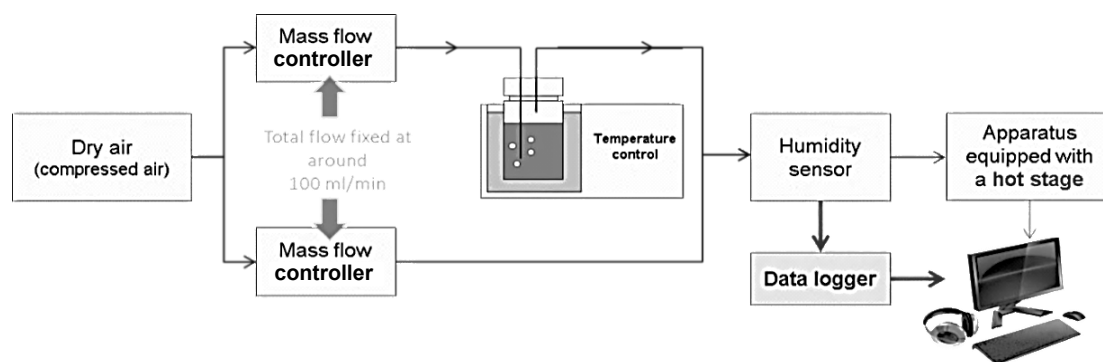


Figure 1. Representation of the humidification system adapted to the material characterization techniques to simulate the practical conditions of seasonal heat storage

2.3. X-Ray Powder Diffraction

In-situ X-ray powder diffraction (XRD) measurements were carried out to identify the variations in composition and crystal structure of the salt hydrates during their dehydration and hydration reactions. The XRD patterns were collected using a Bruker D8 Advance with a MRI oven with Cu $K\alpha_1+K\alpha_2=1.5418 \text{ \AA}$ radiation. Typical runs were conducted with 2-theta ranging from 10 to 45 degrees using a 0.05 degree 2-theta step with a time step of 2 s. The experimental diffraction patterns were compared with known patterns of magnesium sulphate and magnesium chloride hydrates from the JCPDS-ICDD database [3]. The powder samples were placed on an alumina sample holder inside the oven and exposed to a moist air flow at 13 mbar vapour pressure controlled by the humidification system presented in section 2.2. The samples were dehydrated by increasing the temperature from 25°C to 150°C using a heating rate of 1°C/min. The powder samples were kept at 150°C for 3 h to stabilise the final product of the dehydration. Then, the dehydrated materials were rehydrated again by decreasing the temperature from 150°C to 25°C with a cooling rate of 1°C/min followed by a period of several hours at a constant temperature of 25°C. Diffraction patterns were recorded every 10°C in the dynamic modes (heating and cooling) and every 30 min in the isothermal modes.

2.4. Thermal analyses

Thermal analyses were performed to get information on the dehydration and hydration behaviour of the salt hydrate materials. Two thermal analysis techniques were used in this study: Thermogravimetry (TG) and Differential Scanning Calorimetry (DSC) analyses. TG analysis involves the measurement of mass change as a function of temperature or time, and DSC involves the measurement of heat enthalpy changes as a function of temperature or time. The thermal analysis experiments described in this work were performed with a Simultaneous Thermal Analyses apparatus Netzsch STA 409 PC Luxx with a standard SiC furnace, which performs TG and DSC measurements simultaneously. Both dehydration and hydration measurements were carried out at atmospheric pressure (1 atm) by exposing the 10 mg sample to the moist air flow as explained in section 2.2. The sample pans used during these experiments were aluminium cups of 25 μl without lids. The temperature program was adjusted for each material. For $\text{MgSO}_4 \cdot 7\text{H}_2\text{O}$, the dehydration was carried out between 25°C and 150°C with a heating rate of 0.5°C/min and left for 3h hour at 150°C to stabilise the composition of the dehydrated material. Next, the material was rehydrated by a slow cooling at 0.5°C/min until 25°C and subsequently left in isothermal mode at 25°C for 100h. For $\text{MgCl}_2 \cdot 6\text{H}_2\text{O}$, the dehydration was carried out with a heating rate of 0.5°C/min until 130°C. This temperature was chosen since previous measurements [4,5] showed the decomposition of $\text{MgCl}_2 \cdot 2\text{H}_2\text{O}$ above 130°C. The rehydration of the dehydrated material was performed with a cooling rate of 0.2°C/min until 40°C, after which the material was kept isothermal at this temperature to avoid overhydration (see section 3.2.1). The reaction enthalpy and energy density of the phase transition observed during the dehydration and hydration reactions for each salt hydrate were calculated to quantify the heat storage capacity of the material over a reversible sorption cycle.

3. Results and Discussion

3.1. Study on magnesium sulphate heptahydrate

3.1.1 Structural characterization. The diffractograms in figure 2 and figure 3 present the results of the *in-situ* XRD analyses of the dehydration and rehydration reactions of magnesium sulphate heptahydrate ($\text{MgSO}_4 \cdot 7\text{H}_2\text{O}$) under 13 mbar vapour pressure performed with heating and cooling rates of 1°C/min. For the dehydration reaction (figure 2), two structural changes of the material can be observed. First, the initial crystalline phase of magnesium sulphate heptahydrate $\text{MgSO}_4 \cdot 7\text{H}_2\text{O}$ is dehydrated to the crystalline phase of magnesium sulphate hexahydrate $\text{MgSO}_4 \cdot 6\text{H}_2\text{O}$ between 30°C and 40°C. Next, the crystalline phase of $\text{MgSO}_4 \cdot 6\text{H}_2\text{O}$ is slowly decomposed between 60°C and 80°C into an amorphous phase represented by a featureless XRD pattern. The material remains in this state until the end of the dehydration. The absence of lower crystalline hydrated phases of magnesium

sulphate $\text{MgSO}_4 \cdot x\text{H}_2\text{O}$ ($x = 4, 2.5, 2, 1$) and the formation of the amorphous phase have been found in previous studies on the dehydration of magnesium sulphate heptahydrate performed under water vapour pressures below 20 mbar [6,7]. This phenomenon has been attributed to a very slow rate of reaction when the dehydration is performed at 13 mbar [6]. The slow rate of reaction is related to a slow and inhomogeneous reorganization of the crystal structure in the dehydrated material, forming a disordered arrangement of the crystal constituents (atoms, molecules, ions). This molecular arrangement corresponds to an amorphous phase like the structure found for glass.

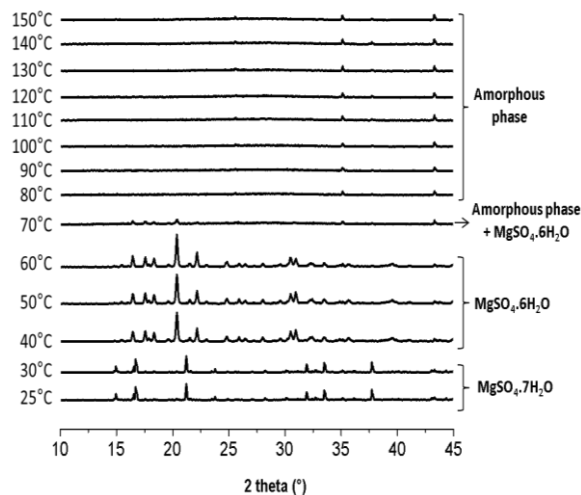


Figure 2. *In-situ* XRD patterns of the dehydration reaction of $\text{MgSO}_4 \cdot 7\text{H}_2\text{O}$ performed between 25 and 150°C under a water vapour pressure atmosphere of 13 mbar with a heating rate of 1°C/min.

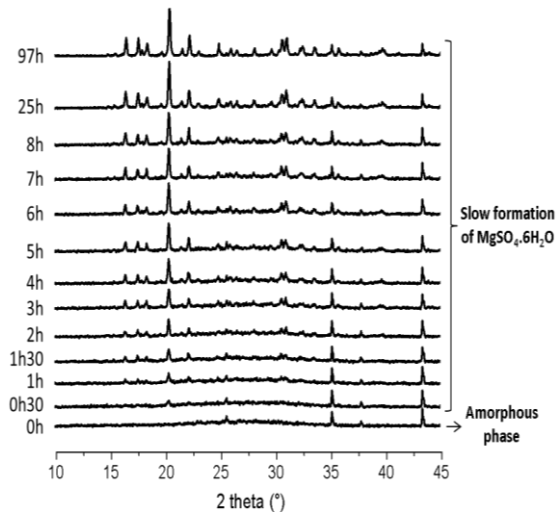


Figure 3. *In-situ* XRD patterns of the hydration reaction of the dehydrated $\text{MgSO}_4 \cdot 7\text{H}_2\text{O}$ performed at the constant temperature of 25°C under a water vapour pressure atmosphere of 13 mbar.

During the rehydration process, the molecular structure of the dehydrated material remains amorphous during the cooling of the system to 25°C and only starts to recrystallize during the isothermal step at 25°C as shown on the XRD pattern in figure 3. After 30 min of isothermal reaction, the characteristic peaks of the crystalline phase of $\text{MgSO}_4 \cdot 6\text{H}_2\text{O}$ appear and the intensities and the sharpness of these peaks slowly increase until 97 h of reaction. However, the phase of $\text{MgSO}_4 \cdot 7\text{H}_2\text{O}$ never appears during this measurement. This result is in agreement with the study performed by Chipera and *al.* [8] on the crystallization of magnesium sulphate hydrates, indicating that the formation of the crystalline phase of $\text{MgSO}_4 \cdot 7\text{H}_2\text{O}$ can only be formed if the ambient water vapour pressure is above 60 mbar. If the water vapour pressure is fixed at 13 mbar, as in seasonal heat storage systems, the phase of $\text{MgSO}_4 \cdot 7\text{H}_2\text{O}$ will never be formed again.

3.1.2 Thermal analyses. The thermal analysis measurements (TG-DSC) of the dehydration and rehydration reactions of magnesium sulphate heptahydrate carried out under 13 mbar water vapour pressure are presented in figure 4 and figure 5. The data of the onset temperature, the reaction enthalpy, and the energy density of each phase transition observed in the dehydration and hydration reaction determined from the DSC measurements are summarized in the table 1.

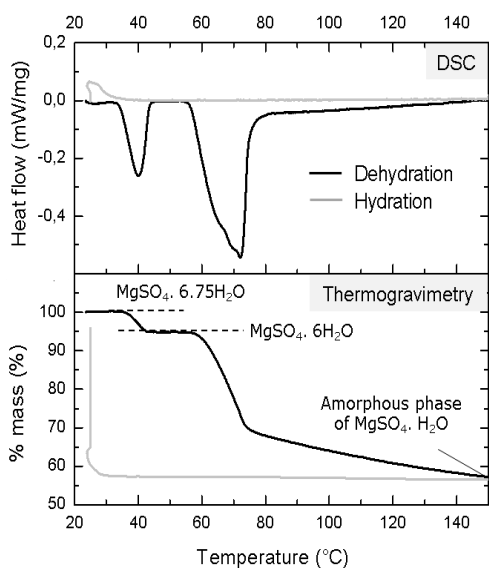


Figure 4. DSC and TG measurements of the dehydration and hydration of $\text{MgSO}_4 \cdot 7\text{H}_2\text{O}$ (heating and cooling rates of $0.5^\circ\text{C}/\text{min}$, $P(\text{H}_2\text{O}) = 13 \text{ mbar}$).

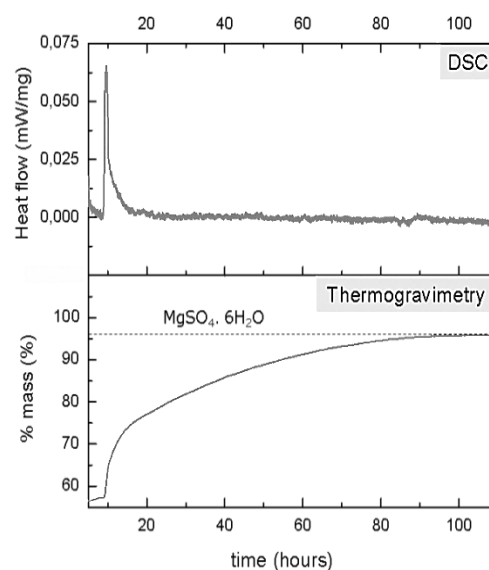


Figure 5. DSC and TG measurements of the hydration reaction of the dehydrated $\text{MgSO}_4 \cdot 7\text{H}_2\text{O}$ (isothermal at 25°C , $P(\text{H}_2\text{O}) = 13 \text{ mbar}$).

The results of these TG-DSC measurements are similar to the results of the XRD analysis. For the dehydration reaction, the DSC and TG curves in figure 4 present two endothermic peaks in the temperature ranges of $35\text{--}45^\circ\text{C}$ and $55\text{--}150^\circ\text{C}$ corresponding to mass losses of 0.75 and 5 water molecules. The first endothermic peak corresponds to the phase transition of $\text{MgSO}_4 \cdot 7\text{H}_2\text{O}$ to $\text{MgSO}_4 \cdot 6\text{H}_2\text{O}$ observed in the XRD measurements presented in section 3.1.1. The lower hydrated composition of $\text{MgSO}_4 \cdot 6.75\text{H}_2\text{O}$ identified on the TG curve (figure 4) signifies that the initial material of the reaction was already partially dehydrated before the measurement. This phenomenon can be explained by the fact that the transition of $\text{MgSO}_4 \cdot 7\text{H}_2\text{O}$ to $\text{MgSO}_4 \cdot 6\text{H}_2\text{O}$ starts at 34°C under these experimental conditions (table 1), which is close to the ambient temperature. Therefore, during the storage and the preparation (sieving) of the material before the measurement, around 25% of the initial $\text{MgSO}_4 \cdot 7\text{H}_2\text{O}$ powder was dehydrated in $\text{MgSO}_4 \cdot 6\text{H}_2\text{O}$. The second endothermic peak of the dehydration corresponds to the dehydration of $\text{MgSO}_4 \cdot 6\text{H}_2\text{O}$ in an amorphous phase (XRD results in section 3.1.1). The TG result presented in figure 4 allows determining that the final composition of this amorphous phase at 150°C is a monohydrated magnesium sulphate. The reversible hydration process of the monohydrated compound begins when the material is cooled below 30°C as shown in figure 4. The rehydration reaction progresses very slowly in a single step during the isothermal process set at 25°C under a water vapour pressure of 13 mbar. After 90 h, the material is fully rehydrated to $\text{MgSO}_4 \cdot 6\text{H}_2\text{O}$. However, it can be observed on the DSC signal in figure 5, that the rehydration of the material only releases heat significantly in the first ten hours of the reaction.

Table 1 shows that the reversible reaction of $\text{MgSO}_4 \cdot 6\text{H}_2\text{O}$ into the amorphous monohydrated phase of magnesium sulphate proceeds at different temperatures during the dehydration and hydration process. However, with the slow rate of heating and cooling of $0.5^\circ\text{C}/\text{min}$ applied to the system during this measurement, it can be assumed that either the reaction takes place under experimental conditions nearby the thermodynamic equilibrium or the reaction is extremely slow. Possibly, external parameters to the thermodynamic properties of the material influence the kinetics of the processes. The hysteresis found in this measurement may be influenced by a possible temperature difference between the surrounding gas and the material caused by the heat effect (exothermic/endothermic) of the reactions.

Table 1. Thermodynamic properties determined from the TG-DSC measurements performed on MgSO₄.7H₂O at 13 mbar with heating and cooling rates of 0.5°C/min

Reactions	T _{onset} [°C]	*ΔrH [kJ/mol]	** Crystal energy storage density [GJ/m ³]
Dehydration			
MgSO ₄ . 6.75H ₂ O(s) → MgSO ₄ . 6H ₂ O(s) + 0.75H ₂ O(g)	34	42.09	0.29
MgSO ₄ . 6H ₂ O(s) → MgSO ₄ . H ₂ O(s) + 5H ₂ O(g)	56	243.81	1.69
Hydration			
MgSO ₄ . H ₂ O(s) + 5H ₂ O(g) → MgSO ₄ . 6H ₂ O(s)	30	110.00	0.76

Reaction enthalpy (*) and crystal energy storage density (**) data are calculated with the molar mass of MgSO₄.6.75H₂O at 241.87 g/mol and the density of MgSO₄.7H₂O or MgSO₄.6H₂O at 1680 kg/m³.

The reaction enthalpies of each chemical reaction observed during the reversible water vapour sorption process were calculated from the DSC results with respect to the molar mass of MgSO₄.6.75H₂O. The results presented in table 1, show that this material is able to store 285.9 kJ/mol during the dehydration reaction with 42.09 kJ/mol for the transition of MgSO₄.6.75H₂O to MgSO₄.6H₂O and 243.81 kJ/mol for the dehydration of MgSO₄.6H₂O into the amorphous monohydrated phase of magnesium sulphate. However, only 110 kJ/mol of the heat is released during the rehydration of the monohydrated phase into MgSO₄.6H₂O, which corresponds to 45% of the energy stored from the dehydration reaction of MgSO₄.6H₂O. Several explanations were proposed in the literature to explain this difference of heat quantified during the two processes. The first explanation may be attributed to the structural modification of the material when the crystalline phase of MgSO₄.6H₂O is dehydrated into the amorphous monohydrate. In a similar study carried out by Bevers and *al.* [9] on the reversible absorption process of ammonia into magnesium chloride, it was concluded that the amorphous state of the material is less capable of absorbing gas than a crystalline structure, resulting in a lower heat effect during the measurements. The heat difference may be also attributed to the textural modifications of the material (cracks, volume expansion) during the reversible water vapour sorption process [10]. During the hydration process, part of the stored heat may be converted in energy to modify the material structure when the water molecules are introduced again in the molecular structure. Additionally, the textural changes of the material will have a direct influence on the experimental conditions during the measurement. The salt may change in a more porous and expanded structure, resulting in a decrease of the contact area between the material and the crucible and lead to a lower recorded heat of transition. A last explanation attributed to a DSC measurement artefact was proposed to explain the heat difference between the dehydration and hydration process. The dehydration is an endothermic reaction where the heat taken up by the material is collected through the sensor of the DSC apparatus, while the hydration is an exothermic reaction where a part of the heat may also be transferred to the surrounding gas phase, reducing the part of the heat collected by the sensor. Although the first explanation proposed seems to be the most likely one for MgSO₄.7H₂O, the others explanations should not be ignored.

In term of energy density, magnesium sulphate heptahydrate presents an energy density of 0.76 GJ/m³ at the end of the cycling test at 13 mbar for a bulk system. This means that for a packed bed reactor of salt hydrate designed for seasonal heat storage with around 50% of porosity [11], magnesium sulphate heptahydrate would release only 0.38 GJ/m³. It can be concluded from this work, that the energy density of magnesium sulphate heptahydrate is too low to fulfil the winter heat demand of an individual house by seasonal heat storage with a 6 m³ packed bed reactor. A minimum volume of 16 m³ would be required for a system set up with MgSO₄.7H₂O.

3.2. Study on magnesium chloride hexahydrate

3.2.1. *Structural characterization.* Previous studies carried out on $\text{MgCl}_2 \cdot 6\text{H}_2\text{O}$ have shown that this material has promising potential as TCM material for seasonal heat storage in term of energy density and temperature release [5,11]. However, this material has some disadvantages for long term storage due to instability and decomposition of the material. At ambient temperature, the material tends to overhydrate into a solution of magnesium chloride. If the overhydrated material is dehydrated again, an impervious layer is formed. This layer causes a reduction of the water vapour transfer in the system which slows down the reaction. In addition, at high temperature around 150°C , the material decomposes into magnesium hydroxychloride MgOHCl , involving a release of hydrochloric acid vapours. This reaction reduces the quantity of active material over time and can induce corrosion on the heat storage system. In order to determine the temperature range over which $\text{MgCl}_2 \cdot 6\text{H}_2\text{O}$ remains in an stable hydrated state during its dehydration and hydration reactions, in-situ XRD measurements have been carried out under a vapour pressure of 13 mbar. The results are presented in figure 6 and in figure 7.

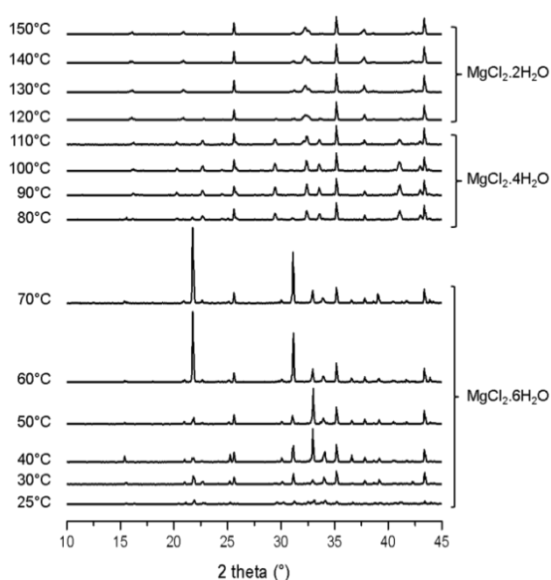


Figure 6. In-situ XRD patterns of the dehydration reaction of $\text{MgCl}_2 \cdot 6\text{H}_2\text{O}$ performed between 25 and 150°C ($p(\text{H}_2\text{O})=13$ mbar, heating rate $1^\circ\text{C}/\text{min}$).

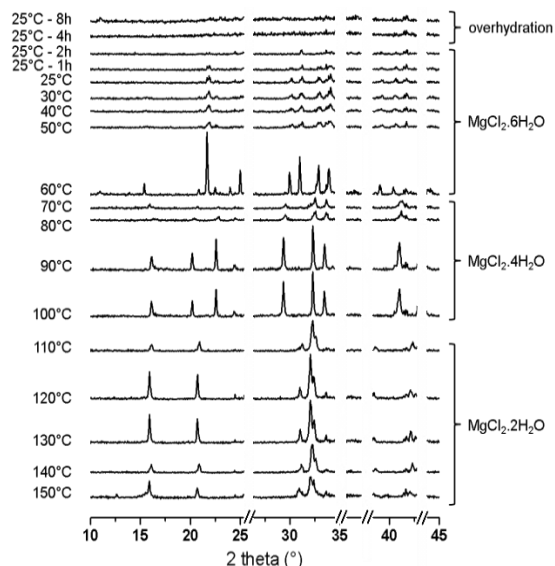


Figure 7. In-situ XRD patterns of the rehydration reaction of $\text{MgCl}_2 \cdot 6\text{H}_2\text{O}$ performed between 150 and 25°C ($p(\text{H}_2\text{O})=13$ mbar, cooling rate $1^\circ\text{C}/\text{min}$).

As shown in figure 6, the initial material used in this experiment presents the characteristic XRD pattern of $\text{MgCl}_2 \cdot 6\text{H}_2\text{O}$. However, the peak intensities on the diffractogram performed at 25°C are very weak due to the overhydration of the material at this temperature. The intensity of the peak increases slowly when the material is heated up until 40°C and the characteristic XRD pattern of the crystalline $\text{MgCl}_2 \cdot 6\text{H}_2\text{O}$ phase remains the same until 50°C . This result is in agreement with the equilibrium conditions T - $p(\text{H}_2\text{O})$ determine by Siegesmund and *al.* [12] indicating that $\text{MgCl}_2 \cdot 6\text{H}_2\text{O}$ remains in solid state for a temperature above 30°C in combination with a water vapour pressure of 13 mbar. Between 60°C and 70°C , the XRD patterns keep the peak distribution of the crystalline phase of $\text{MgCl}_2 \cdot 6\text{H}_2\text{O}$ but the intensities of certain peaks are modified. In XRD analyses, the increase or decrease of the intensity of the peak, as shown for the peak at 21.75° , are explained by a preferential orientation of the material during the measurement. Therefore, in this experiment the variation of the peak intensities for a same phase $\text{MgCl}_2 \cdot 6\text{H}_2\text{O}$ may be attributed to a modification of the grains orientation in the powder sample in this temperature range of 60 - 70°C which foregoes the first step of dehydration of the material. Indeed, the dehydration reaction of $\text{MgCl}_2 \cdot 6\text{H}_2\text{O}$ until 150°C performed

with 1°C/min presents two steps of dehydration with the formation of the crystalline phases of $\text{MgCl}_2 \cdot 4\text{H}_2\text{O}$ in the temperature range of 80-110°C and of $\text{MgCl}_2 \cdot 2\text{H}_2\text{O}$ in the temperature range of 120-150°C indicated by very well-defined XRD patterns in figure 6. No XRD peaks characteristic of the crystalline phase of magnesium hydroxychloride MgClOH have been observed on the spectra at 150°C after 3h of isothermal process, which means that magnesium chloride remains as a salt hydrate material after one cycle under the seasonal heat storage conditions ($T_{\text{max}} = 150^\circ\text{C}$, 13 mbar). During the rehydration process shown in figure 7, the crystalline phase of $\text{MgCl}_2 \cdot 2\text{H}_2\text{O}$ is rehydrated in the crystalline phases of $\text{MgCl}_2 \cdot 4\text{H}_2\text{O}$ when the system is cooled down below 100°C and $\text{MgCl}_2 \cdot 6\text{H}_2\text{O}$ when the temperature reaches 60°C. In this measurement, it is shown once again that $\text{MgCl}_2 \cdot 6\text{H}_2\text{O}$ remains in a solid state until 30°C and slowly liquefies at 25°C to form a solution of magnesium chloride.

3.2.2. Thermal analyses. The thermal analysis (TG-DSC) performed during the dehydration and rehydration reactions of $\text{MgCl}_2 \cdot 6\text{H}_2\text{O}$ was carried out under 13 mbar water vapour pressure. The temperature of rehydration was limited to a minimum of 40°C to avoid the overhydration of the material at ambient temperature and a maximum temperature of the dehydration was fixed at 130°C. The dehydration and hydration reaction were carried out with a heating rate of 0.5°C/min and a cooling rate of 0.2°C/min. Figure 8 and figure 9 present respectively the TG and DSC results obtained during these measurements. Additionally, the data of the onset temperature, the reaction enthalpy, and the energy density determined from the DSC measurements have been summarized in table 2.

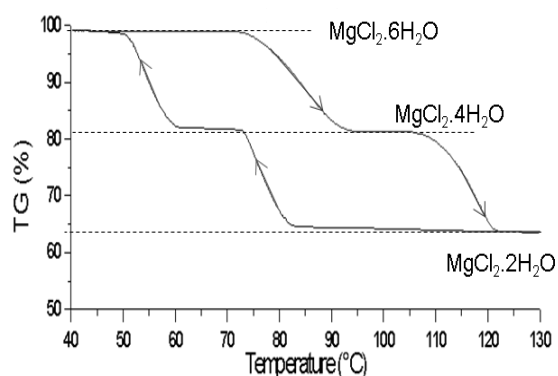


Figure 8. TG measurements of dehydration and hydration reactions of $\text{MgCl}_2 \cdot 6\text{H}_2\text{O}$ performed under a water vapour pressure of 13 mbar with a heating rate of 0.5°C/min and a cooling rate with 0.2°C/min.

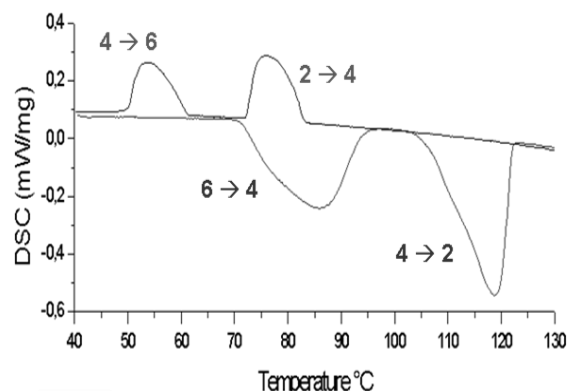


Figure 9. DSC curve of dehydration and hydration reactions of $\text{MgCl}_2 \cdot 6\text{H}_2\text{O}$ performed under a water vapour pressure of 13 mbar with a heating rate of 0.5°C/min and a cooling rate with 0.2°C/min.

The TG-DSC measurements performed on $\text{MgCl}_2 \cdot 6\text{H}_2\text{O}$ show similar results as the results obtained by XRD measurements. As shown on the TG curve in figure 8, magnesium chloride hexahydrate is dehydrated in two consecutive steps with a loss of two water molecules for each step between 75-95°C and 105-123°C under the experimental conditions set in this experiment (0.5°C/min, 13 mbar). These two mass losses are accompanied by two corresponding endothermic peaks on the DSC curve in figure 9, corresponding to the formation of the lower hydrated phases $\text{MgCl}_2 \cdot 4\text{H}_2\text{O}$ and $\text{MgCl}_2 \cdot 2\text{H}_2\text{O}$. The final $\text{MgCl}_2 \cdot 2\text{H}_2\text{O}$ phase keeps a stable composition at 130°C when the material remains in an isothermal step for 1 h. The rehydration of $\text{MgCl}_2 \cdot 2\text{H}_2\text{O}$ proceeds during the cooling of the material as shown on the TG curve (figure 8) with the formation of $\text{MgCl}_2 \cdot 4\text{H}_2\text{O}$ below 83°C and of $\text{MgCl}_2 \cdot 6\text{H}_2\text{O}$ below 61°C. After an isotherm of 3h at 40°C, the phase of $\text{MgCl}_2 \cdot 6\text{H}_2\text{O}$ formed at the end of the dehydration/hydration cycle remains as a solid without trace of overhydration of the material. Therefore, it would be recommended for a seasonal heat storage system based on the reversible water vapour sorption process of $\text{MgCl}_2 \cdot 6\text{H}_2\text{O}$ to set the minimum temperature of the hydration process at 40°C to avoid the overhydration of the material.

Table 2. Thermodynamic properties determined from the TG-DSC measurements on $\text{MgCl}_2 \cdot 6\text{H}_2\text{O}$ at 13 mbar with an heating rate of $0.5^\circ\text{C}/\text{min}$ and a cooling rate of $0.2^\circ\text{C}/\text{min}$

Reactions	T_{onset} [$^\circ\text{C}$]	* ΔrH [kJ/mol]	** Crystal energy storage density [GJ/m ³]
Dehydration			
$\text{MgCl}_2 \cdot 6\text{H}_2\text{O} (\text{s}) \rightarrow \text{MgCl}_2 \cdot 4\text{H}_2\text{O} (\text{s}) + 2\text{H}_2\text{O} (\text{g})$	71	102.61	0.78
$\text{MgCl}_2 \cdot 4\text{H}_2\text{O} (\text{s}) \rightarrow \text{MgCl}_2 \cdot 2\text{H}_2\text{O} (\text{s}) + 2\text{H}_2\text{O} (\text{g})$	105	117.41	0.90
Hydration			
$\text{MgCl}_2 \cdot 2\text{H}_2\text{O} (\text{s}) + 2\text{H}_2\text{O} (\text{g}) \rightarrow \text{MgCl}_2 \cdot 4\text{H}_2\text{O} (\text{s})$	83	102.73	0.79
$\text{MgCl}_2 \cdot 4\text{H}_2\text{O} (\text{s}) + 2\text{H}_2\text{O} (\text{g}) \rightarrow \text{MgCl}_2 \cdot 6\text{H}_2\text{O} (\text{s})$	61	81.10	0.62

Reaction enthalpy (*) and crystal storage energy density (**) data are calculated with the molar mass and the density of $\text{MgCl}_2 \cdot 6\text{H}_2\text{O}$ at 203.31 g/mol and 1560 kg/m³.

The shift of the onset temperature (table 2) and the formation of a hysteresis on the TG curve in figure 8 both lead to the same conclusions as previously found for magnesium sulphate heptahydrate. The kinetics of the water vapour sorption process of $\text{MgCl}_2 \cdot 6\text{H}_2\text{O}$ are controlled by the surrounding water vapour pressure and the temperature applied to the system. In this measurements performed under a constant water vapour pressure of 13 mbar with low heating and cooling rates, the phenomenon may be attributed to the temperature difference between the surrounding gas and the material caused by the heat effect of the dehydration and hydration reactions. The reaction enthalpies were determined for each chemical reaction observed during the dehydration/hydration cycle of $\text{MgCl}_2 \cdot 6\text{H}_2\text{O}$ from the DSC curves (table 2). As observed previously for magnesium sulphate (section 3.1.2), the heat released from the material during the hydration process is lower than the heat stored in the material during the dehydration. The heat released from the chemical reactions $\text{MgCl}_2 \cdot 2\text{H}_2\text{O}$ to $\text{MgCl}_2 \cdot 4\text{H}_2\text{O}$ and $\text{MgCl}_2 \cdot 4\text{H}_2\text{O}$ to $\text{MgCl}_2 \cdot 6\text{H}_2\text{O}$, corresponds respectively to 87% and 79% of the heat stored during the dehydration reaction. These values are higher than those obtained for the hydration reaction of magnesium sulphate. These results tend to confirm the explanation proposed for magnesium sulphate heptahydrate (section 3.1.2) which attributes the low release of the heat during the hydration reaction to the amorphization of the material. In the case of $\text{MgCl}_2 \cdot 6\text{H}_2\text{O}$, the textural changes in the material and heat losses to the gas proposed in section 3.1.2. should be taken in consideration. In fact in this measurement, the heat loss effect into the gas was increased by the fact that the cooling rate ($0.2^\circ\text{C}/\text{min}$) applied to the system for the hydration in this measurement was slower than the heating rate ($0.5^\circ\text{C}/\text{min}$) of the dehydration process.

In terms of energy density, magnesium chloride hexahydrate presents a total energy density of 1.41 GJ/m³ at the end of the cycling test at 13 mbar for a bulk system. This means that for a packed bed reactor designed for seasonal heat storage with 50% of porosity, magnesium chloride hexahydrate would release 0.71 GJ/m³. Therefore, $\text{MgCl}_2 \cdot 6\text{H}_2\text{O}$ can fulfil the winter heat demand of an individual house with a packed bed reactor of 8.5 m³, which means that this material is almost five times more compact than seasonal heat storage in a water tank. This material presents promising characteristics as TCM material for this application.

4. Conclusion

The investigation of the reversible water vapour sorption process of $\text{MgSO}_4 \cdot 7\text{H}_2\text{O}$ and $\text{MgCl}_2 \cdot 6\text{H}_2\text{O}$ under seasonal heat storage conditions showed that the thermodynamic and kinetic properties of these materials are directly related to the structural and textural modifications undergone by the materials during their dehydration and hydration reactions. These modifications are controlled by the water vapour pressure set at 13 mbar for a seasonal heat storage system, the temperature of dehydration and hydration and the rate of heating and cooling applied to the system during these reactions.

In this study, it was found that under a water vapour pressure of 13 mbar, $\text{MgSO}_4 \cdot 7\text{H}_2\text{O}$ dehydrates into an amorphous monohydrate phase when the system is heated until 150°C and rehydrates after

100 h by recrystallizing the crystalline phase of $\text{MgSO}_4 \cdot 6\text{H}_2\text{O}$. The material is able to take up 0.99 GJ/m^3 of heat for a packed bed built with 50% of porosity during the dehydration of the material. However, it only released 0.38 GJ/m^3 of heat during the rehydration process. This low heat release is mainly attributed to the amorphization of the material during the dehydration performed at 13 mbar which reduces its sorption capacity during the rehydration. Nevertheless, the low heat release may also be assigned to textural changes which influence the measurement conditions. Additionally, experimental artefacts of the DSC measurements may influenced the heat storage capacity found for this material. $\text{MgCl}_2 \cdot 6\text{H}_2\text{O}$ presents a much lower difference between its stored energy density of 0.84 GJ/m^3 and its heat release of 0.71 GJ/m^3 . For this material, XRD results showed that the phases $\text{MgCl}_2 \cdot 4\text{H}_2\text{O}$ and $\text{MgCl}_2 \cdot 2\text{H}_2\text{O}$ found during the dehydration and hydration of this material were crystalline. The small difference in hydration and dehydration enthalpies may be attributed to the textural changes in the material and experimental artefacts. The high heat storage capacity of $\text{MgCl}_2 \cdot 6\text{H}_2\text{O}$ means that this material can fulfil the winter heat demand of a passive house estimated at 6 GJ with a packed bed reactor of 8.5 m^3 . This volume is almost five times smaller than a water tank used for latent seasonal storage. $\text{MgCl}_2 \cdot 6\text{H}_2\text{O}$ presents definitively a promising means for seasonal heat storage in for individual dwelling. Nevertheless, a seasonal heat storage system based on the water vapour sorption process in $\text{MgCl}_2 \cdot 6\text{H}_2\text{O}$ should be carefully set with a restricted temperature of 40°C for the hydration reaction to avoid the liquefaction of the material at ambient temperature, since this would limit the performance of the material for long term storage.

Acknowledgments

This research has been performed in cooperation between ECN and the Mechanical Engineering group of the University of Eindhoven (TU/e). The project has received financial support from the Advanced Dutch Energy Material (ADEM) program. The authors would like to thank Vera Smit-Groen (NRG) for performing the X-ray diffraction experiments and Gertjan Herder (ECN) for his contribution in the TG-DSC experiments.

Reference

- [1] van Essen V M, Bleijendaal L P J, Cot Gores J, Zondag H A, Schuitema R, van Helden W G J, He Z and Rindt CCM 2009 *Proc. Int. Conf. 11th on Thermal Energy Storage for Efficiency and Sustainability (Stockholm, Sweden, 14–17 June 2009)* p 14
- [2] van Essen V M, Zondag H A, Cot Gores J, Bleijendaal L P J, Bakker M, Schuitema R, van Helden W G J 2009 *J. Sol. Energy Engineering* **131** 041014
- [3] Powder Diffraction File 2005 *Int. Cent. for Diffraction Data (Newtown)*
- [4] Opel O, Rammelberg HU, Gerard M and Ruck W 2011 *Proc. Int. Conf. for Sustainable Energy Storage (Belfast, UK, 21–24 February 2011)*
- [5] H.A. Zondag, B.W.J. Kikkert, S. Smeding and M. Bakker 2010 *Proc. Int. Conf. 5th on Renewable Energy Storage (Berlin, Germany, 22-24 November 2010)*
- [6] Wattle-Marion G, Lallemand M and Bertrand G 1972 *Proc. Int. Symp. 7th on the Reactivity of Solids (Bristol, UK, 17–21 July 1972)* 772
- [7] L'vov BV 2007 *Thermal Decomposition of Solids and Melts – New thermochemical approach to the mechanism, kinetics and methodology* (Berlin : Springer) 100
- [8] Chipera S J and Vaniman D T 2006 *Geochim. Cosmochim. Acta* **71** 241
- [9] Bevers E R T, Onnk H A J, Haije W G and van Ekeren P J 2007 *J. Therm. Anal. Calorim.* vol 90 **3** 923
- [10] Galwey A K and Brown M E 1999 *Thermal decomposition of ionic solids* (Amsterdam: Elsevier) 217
- [11] Zondag H A, Kikkert B W J, Smeding S and Bakker M 2011 *Proc. Int. Conf. for Sustainable Energy Storage (Belfast, UK, 21–24 February 2011)*
- [12] Siegesmund S and Snelthlage R 2011 *Stone in Architecture: Properties, Durability 4th Edition*, (Berlin: Springer)